
ISSN: 2321-2152
IJMECE
International Journal of modern electronics and communication engineering
E-Mail
editor.ijmece@gmail.com
editor@ijmece.com
www.ijmece.com

IJMECE
International Journal of modern electronics and communication engineering

ISSN 2321-2152
www.ijmece.com
Vol 13, Issue 2, 2025

Enhancing Grid Power Quality With a PV-Based NPC Multilevel Inverter And Active Filtering

[1]Dr. M. Bhaskar Naik,[2]Posa Mahalakshmi, [3]Sake Kesava, [4]Eddula Riya Sultana, [5]Varakuti Sunanda,

[1]Associate Professor, Department Of EEE, Ananthalakshmi Institute Of Technology And Sciences, Itikalapalli, Near Sk University,Ananthapur,

[2,3,4,5] Student, Department Of EEE, Ananthalakshmi Institute Of Technology And Sciences, Itikalapalli, Near Sk University,Ananthapur.

ABSTRACT

This study proposes a three-phase Shunt Active Power Filter (SAPF) that is based on a photovoltaic (PV) interface and uses a Neutral Point Clamped (NPC) voltage source inverter. At first, we cover the most important power quality concerns, including reactive power compensation, reducing source current Total Harmonic Distortion (THD), increasing power factor, and integrating the energy from the PV system into the electrical power grid. To solve power quality problems, a multilayer NPC inverter-based SAPF was later created using the Adaptive Neuro Fuzzy Inference System (ANFIS) algorithm and Synchronous Reference Frame Theory (SRF). Using the SRF theory, we determine the reference current needed for compensation, and then we use the ANFIS algorithm to create a DC link voltage that is smooth. To further decrease the transient harmonic distortion (THD) caused by balanced or unbalanced nonlinear (NL) loads, a hysteresis current controller (HCC) is used to provide the necessary switching pulses to the neutral point clamped voltage source inverter. Power from photovoltaic (PV) arrays is put to good use by the SAPF. To optimize the power extraction from PV arrays into the electrical grid, it uses an MPPT controller based on Enhanced Incremental Conductance (EINC). In addition to enhancing grid power quality by the elimination of harmonics, it also enables load-reactive power demand. Hardware and MATLAB simulation are used to verify the performance of the proposed system. In both balanced and unbalanced NL load scenarios, the experimental findings show that the suggested system performs better by reducing harmonics and keeping the DC link voltage constant.

INDEXTERMS
Neutralpointclampedconverter,FPGA,powerquality, photovoltaic system, ANFIS, shunt active power filter.

INTRODUCTION

The present state of centralized electric energy generation is insufficient to fulfill the ever-increasing demand for power. Research into energy production is vital because of the influence it has on the development of economies throughout the world. Governments, organizations, and people alike are very interested in and concerned about this issue, which covers a broad spectrum of technology and methods [1, 2]. This area requires Jorge Esteban Rodas Benítez was the assistant editor who oversaw the manuscript's assessment and gave the final approval for publication. The difficulty of producing energy in a safe, efficient, and sustainable manner necessitates ongoing study and novel solutions. In order to meet the ever-increasing need for energy, many nations and businesses invest heavily in traditional power plants that run on coal, diesel, or gas. But their astronomical costs, lack of efficiency, and negative impact on the environment are slowly limiting their use. There is general agreement that increased carbon dioxide emissions, climate change, and environmental damage are outcomes of massive industrial output.
Future energy production is jeopardized since this process causes natural resources to be depleted. Since these sources of power are constantly refilling themselves, some countries have turned to green energy and other forms of renewable energy. The energy sources indicated above are considered ecologically beneficial and do not add to the problem of global warming [3, 4, 5, 6]. Some renewable energy technologies have more promise than others; one such technology is distributed energy resources based on photovoltaic (PV) systems. In most parts of

the globe, PV systems can produce an endless amount of electricity, and they are also very efficient and dependable [7]. They have been especially helpful in ensuring that remote areas and towns have access to a steady supply of electricity. Additionally, they assist nations who do not produce oil in reducing the costs of energy and production imports, which in turn lowers consumption bills. Additionally, researchers are motivated to improve the manufacturing processes of superior PV systems because of the environmental friendliness of these systems, which is shown by their absence of pollutant emissions. Innovative photovoltaic (PV) systems may soon play a pivotal role in meeting global energy needs while lowering pollution levels [8]. Because of the proliferation of non-linear loads connected to the power grid, power quality has emerged as a critical concern in the integration of solar systems with the electrical network. Current and voltage harmonics, power factor, reactive power, and an increasing need for active power are some of the problems that these loads are adding to [9], [10], [11]. A PV panel, power converter (DC-DC), DC-link energy storage, three-level semiconductor avalanche photovoltaic filter (SAPF), grid-connected filter, and controller circuit are all parts of a grid-connected photovoltaic system that work together to solve these problems. Electric power producing systems that include SAPF see a significant improvement in power and current quality, as well as a decrease in costs due to the elimination of the need for routine equipment maintenance. A plethora of NLloads have been introduced as a result of recent substantial advancements in the energy and power industry. But this has changed the electricity quality significantly. To lessen or eliminate the effect of such NL burdens on power equality, many methods have been devised. Passive filters, active power filters in series and parallel, and hybrid active power filters are all examples of such methods [12], [13].

Although AC and DC drives are often used in high-power industrial applications, they may cause unwanted harmonics. Unfortunately, two-level active power filters aren't an option for reducing harmonics produced by high power NLs since the switches used have reverse rating restrictions. Reducing total harmonic distortion (THD), an essential consideration for feeding power into the grid from solar panels, is a big obstacle to grid integration. By using two-level inverters, the SAPF successfully eliminates harmonics and restores reactive power balance [14]. The greater switching frequency of the two-level inverter might present problems for managing the power of improved NLs, hence this solution is usually reserved for low-power NLs. This is due to the fact that inverters' static switches produce substantial switched currents, necessitating the usage of many inverter switches to achieve a desired degree of power efficiency while reducing switched currents, which in turn increases the switch voltage [15]. Connecting the solar system to the electrical system via a multi tilevel inverter is a practical way to overcome this restriction. Fewer harmonic rates, lower switching losses, and improved electromagnet compatibility are only a few of its many advantages [16, [17], [18], [19]. To reduce harmonics in power lines and adjust for reactive power, NPC-based inverter designs are extensively used in high and medium power applications, as described in [20]. These inverters offer a plethora of benefits, such as lowering the amount of harmonics in the output voltage, improving the harmonics in the source current, reducing the voltage stress on power semiconductors, decreasing switching losses, and potentially avoiding problems associated with SAPF-based two-level inverters. Techniques for producing reference current harmonics with excellent tracking quality, dynamic DC bus voltage management, robust and accurate creation of gate-switching pulses, and dynamic and stable injection currents all impact the effectiveness of SAPF using three-level NPC inverters. The effect of pulse width and switching frequency on the performance of three-level NPC inverters has been the subject of several investigations. While regulating the DC bus voltage, the reference current is retrieved as part of the compensation process. Controlling the production of reference current in SAPF is often accomplished using the SRF theory. Another method is the Instantaneous Reactive capacity Theory (IRPT), which unfortunately requires a lot of computing capacity, has a poor reaction time, and isn't ideal for dynamic load variations. An improved power quality distributed static compensator based on photovoltaics is best described in the literature using SRF theory [21]. The operation of any Active Power Filter (APF) is dependent on the control of the inverter DC side capacitor voltage. Conventional wisdom is that the inverter DC side voltage should be controlled using proportional integral (PI) controllers. When dealing with systems that exhibit significant nonlinearity, it might be challenging to get an accurate model, a need for implementing PI controllers. Consequently, several intelligent controllers that do not need exact models have been investigated in the literature. Controls based on Particle Swarm Optimization (PSO), Genetic Algorithms (GA), Fuzzy Logic Controls (FLC), and Artificial Neural Networks (ANNs) are among them. The FLC that Benchouia et al. developed to respond to variations in voltage errors was experimentally verified using DSPACE-1104 [22].

An ANN current controller-based multilayer harmonic filter was simulated and built by Mahajan et al. [23]. An FLC is a part of this filter that controls the inverter's DC-link voltage [24]. Nevertheless, FLC has the drawback of having to handle many fuzzy sets and rules in connection to changes in load. An Adaptive Neuro-Fuzzy Inference System controller is used to manage the DC side capacitor voltage of the inverter, which helps to overcome these restrictions. This controller is able to adapt to changes in the system and combines the features of FLC and ANN controllers [25], [26]. The Multi-Level Inverter (MLI) used in parallel APF is trigged by simple three-level hysteresis current controllers (HCCs). By using MATLAB and proto-type hardware, the functionality of the system is confirmed. The suggested method is an alternative to conventional linear control schemes that use a PI controller; its goal is to improve system stability via efficient management of load variations. The main things that this study accomplished are: 1) Accurately tracking and attaining the maximum power point from the PV module is achieved by the Enhanced Incremental Conductance (EINC) based MPPT controller. 2) To meet the reactive power requirement of the load and provide active power from the PV system, they suggest an EINC-based PV interconnection using a three-level NPC voltage source inverter SAPF. 3) A controller with ANFIS capabilities to maximize PV-SAPF performance under different load conditions while keeping the DC-link capacitor voltage constant. Conversely, the gating signals are more efficiently generated by means of the HCC. 4) To verify the performance of the ANFIS controller, we will compare it to the traditional PI controller in SAPF and examine the results. 5) By integrating SRF theory with HCC, the ANFIS controller improves power quality, meets IEEE 519 requirements, and enhances system performance by dampening harmonics and minimizing source current THD. The second part of the article's structure is this: The second section discusses the SAPF system, which is based on photovoltaics, and describes and models three-level NPC inverters. The system's photovoltaic array, harmonic extraction using SRF theory, and the implementation of an ANFIS controller for managing DC link voltage were all covered in the same section. Under balanced and unbalanced NL load circumstances, the results and discussion of the simulation are presented in section III. The findings of testing a PV-based three-level NPC inverter with SAPF under different hardware loading situations are provided in Section IV. At last, the paper's Section V serves as the research's conclusion.

MODELLING AND DESCRIPTION OF SYSTEMS

As illustrated in Figure 1, the proposed SAPF system for this research is based on PV modules with many levels of inverters. This setup

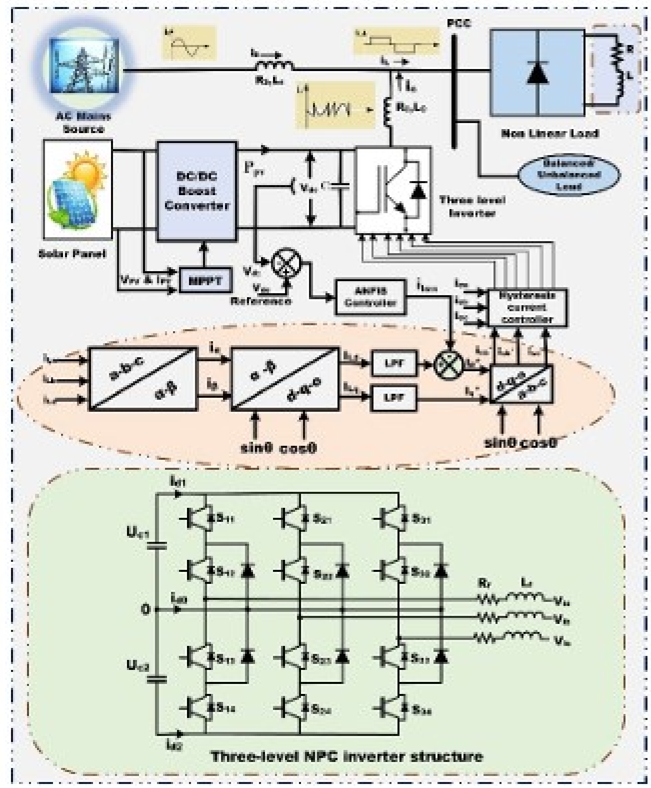

FIGURE 1. Power circuit of diagram of integrated three-level NPC inverter-based PV-SAPF.

comprises a PV module, a DC-DC step-up converter, a SAPF based on amul tilevel inverters, and linked loads. Under all operational conditions, a three-phase, three-level SAPF DC-link may accomplish maximum power factor correction (MPPT) by adjusting its duty cycle based on the output of a DC-DC step up converter. In order to link the SAPF network at the

ISSN 2321-2152
www.ijmece.com
Vol 13, Issue 2, 2025

PCC to the grid and smooth out currents, interface inductors are used. To provide a non-linear load, an inductive load is linked to a three-phase uncontrolled rectifier. The switching pulses are supplied by a three-level HCC, and the multilevel inverter based SAPF is used. Power factor enhancement, harmonic distortion mitigation, reactive power demand support, and active power delivery from a PV system to a load or distribution system may all be achieved by means of this technology. The other components are described briefly below. In addition to the anti-parallel configuration of the transistors and diodes, the three-level NPC inverters include two capacitors connected to the DC bus. These capacitors establish a connection with the reference point (o) and get a medium voltage. There are four bidirectional switches on each inverter arm. With SAPF as the PCC's rent source, the interaction may be explained by the differential equations below [11], [27].

$$\begin{cases} L_f \dfrac{di_{fd}}{dt} = -R_f i_{fd} - L_f \omega i_{fq} + V_{sd} - V_{fd} \\ L_f \dfrac{di_{fq}}{dt} = -R_f i_{fq} - L_f \omega i_{fd} + V_{sq} - V_{fq} \\ C \dfrac{di_{fq}}{dt} = i_{fd} V_{fd} + i_{fq} V_{fq} \end{cases} \quad (1)$$

TABLE 1. Three level inverter switching state

Voltage	States	Current State of Switching Devices (M=1,2,3) (0=OFF,1=ON)			
		S_{M1}	S_{M2}	S_{M3}	S_{M4}
$V_{dc}/2$	P	1	1	0	0
0	O	0	1	1	0
$-V_{dc}/2$	N	0	0	1	1

If one were to apply Kirchhoff's current law to the source current at the PCC point, one would get IS = IF + IL, where IF and IL are the filter currents and load currents, respectively. Here, the reactive and active components of the load current are subject to harmonic limitations by use of the parallel SAPF, which functions as a current generator. To reduce the impact of harmonics in the active-reactive load current, the parallel SAPF acts as a generator of current in this specific case. It is the goal of the system to counteract the load's absorbed harmonic currents by injecting them into the electrical network at the same amplitude but in the opposite phase. The integers '−1', '0', and '1' represent the modes of operation in the switching SMX. For each value, there is an associated arm that is connected to the DC-link capacitor's positive, negative, or neutral terminals. Table displays the values of X as 1, 2, 3, and 4, and M as a, b, and c. 1. provides a catalog of the procedures and their corresponding output voltages. Part A: Photovoltaic The non-linear V-I characteristics of the PV cell change with temperature and solar radiation, as shown in Figure 2. Consequently, it is critical to keep an eye on the maximum power output of the array. Parameters of the PV array (Voc, Isc), solar radiation, temperature, and output parameters (DC link voltage, for example) are all inputs that the MPPTcontroller considers while regulating the boost converter's operation. Traditional incremental and conductance MPPT methods have poor performance in situations when the MPP f luctuates and irradiance conditions vary quickly. We have created an upgraded INC MPPT to overcome these challenges. In order to get the most power out of a step-up converter, this method regulates its duty cycle. The reference article[28, [29], [30] discusses this development option in full. Displayed here is the EINC MPPT method. Image 3. The PV array sends its output to the DC-DC step-up converter. The output of the boost converter is connected to the SAPF's DC bus. A step-up converter boosts the 305.6 V output voltage from the PV array to 750 V. Mathematical models. Below, we can see that the diode and load currents of the PV module are provided by (2) and (3).

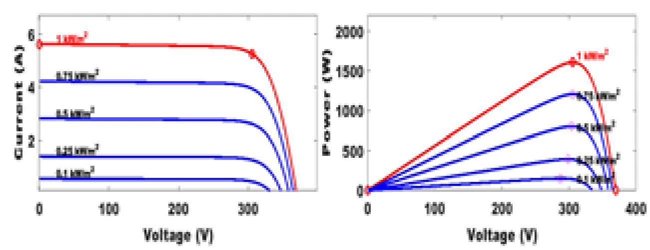

FIGURE 2. Trina solar TM-200DA01A; PV curve for solar PV array voltage vs. and power and voltage vs. current characteristics.

Trina Solar TSM-200DA01A array solar PV modules are used to power the system. Figure 4 shows a comparison of the EINC and INC MPPT methods for maximizing power production from solar systems with respect to temperature and irradiance fluctuations. With respect to dynamic reaction in particular, the EINCalgorithm surpasses the

ISSN 2321-2152
www.ijmece.com
Vol 13, Issue 2, 2025

traditional INC algorithm. When solar radiation is falling, the old technique is less efficient than the new one, and it's much less efficient when radiation is rising.

TABLE 2. Responsibilities carried out by the ANFIS controller layer

Name of the Layer		The Layer Outputs
Layer-1:	Fuzzification Layer	It employs the Sugeno fuzzy rule to translate input physical variables into linguistic variables, demonstrating the adaptive nature of each node (U and V). The work uses error voltage (Er) and change in error voltage (ΔEr) as input variables, denoted by e_1 and e2. The result of this layer, as provided by $L_i^1 = \mu_{V1} E_r$ (11) $L_j^1 = \mu_{V2} \nabla E_r$ (12)
Layer-2:	Product Layer	calculates the degree of applied fuzzy rule by multiplying inputs at each node with a fixed type nature. $L_i^2 = d_i = (\mu_{Ui} E_r) \times (\mu_{Vi} \Delta E_r)$ (13)
Layer-3:	Normalized layer	In this layer's {labeled (N)} nodes are all the fixed nature types. This layer is employed to complete the IF portion of the fuzzy rule and normalize the input degree. The result of this layer is provided by $L_i^3 = \bar{d}_i = \frac{d_i}{\sum_{k=1}^{2} d_k}$ (14)
Layer-4:	Defuzzifier Layer	The fourth layer of the ANFIS architecture features square-shaped, adaptable nodes, each producing MF output based on learning principles. $L_i^4 = d_2 \times f_i = (\bar{d}_i \times (x_i \times E_r + y_i \times \Delta E_r + z_i))$ (15)
Layer-5:	Output Layer	This layer, consisting of a fixed nature type exit node labeled by a summation sign, provides the final part of the fuzzy rule. $L_i^5 = \sum_i (\bar{d}_i \times f_j) = \frac{\sum_i (d_i \times f_i)}{\sum_i^d}$ (16)
Here, the nodes i and j employ the input variables Er and ΔEr.		

SIMULATION RESULTS AND DISCUSSION

A PV-SAPF simulation model is constructed in the MATLAB environment and tested under different load circumstances. Solar panels, non-linear loads, a controller, coupling inductance, three-level inverters, and three-phase alternating current sources are the main components of the model. The parameters and design of the simulation are shown in Table.3. By analyzing its impacts on balanced, unbalanced, and NL loads, the analysis reveals how a combined PV-SAPF system operates. A. The Role of Control in Balanced and Non-Linear State Conditions The distribution system's PCC is linked to a balanced and NLs. Grid voltage, as seen in Figure 7,

TABLE 3. Design the parameters of the simulation

Components	Parameter	Value
Grid	Source voltage (Phase voltage)	230 V,50 Hz
PV Boost converter	PV Module	P_{PV}=200.9W; I_{sc}=5.62 A; V_{oc}=46.2 V; V_m=38.2 V; I_m=5.26 V.
	Boost Converter	L=68.5 mH; C_{in}= 100 µF; V_{pv}=V_{in}=305.6 V; V_{dc}=750 V
Filter	Inductance	5 mH
DC-link voltage	Capacitor	2200µF
Nonlinear load	Resistor and inductor	R=81Ω and L=12mH
Balanced load	Resistive load	R_1= R_2= R_3=110Ω
	Inductive load	160mH
Unbalanced load	Resistive load	R_1=110Ω; R_2=75Ω; R_3=50Ω
Note: V_m , I_m and P_{PV} are maximum power voltage, current and power of PV; Voc and Isc are open-circuit voltage and Short-circuit current.		

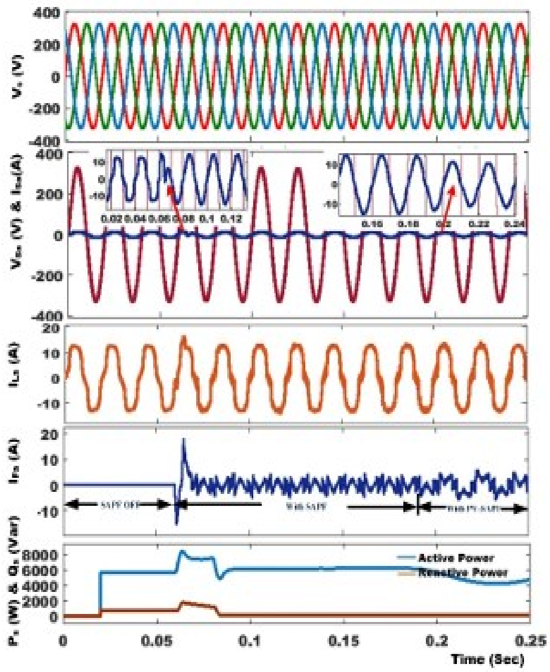

FIGURE 9. System performance of system (a) grid voltage (b) grid voltage and current (c) Load current (d) Filter current (f) Source active and reactive power waveforms.

the source's reactive power. A power factor of unity is guaranteed by synchronizing the addressed source cur values with the source voltage. In order to reduce reactive power demand and harmonics, photovoltaic (PV) is integrated with actual power from SAPF and supplied into the system's load at t=0:18s. Figures.8 and 9.7 show the harmonic spectra before and after source current adjustment, respectively. Reduced from 18.61%, the total harmonic distortion (THD) of the source current is now just 1.26%.

The PCC of the diffusion system is linked to an imbalanced and NL. Power in both active and reactive forms, as well as grid voltage, load current, filter current, and grid voltage and current are shown in Figure 9. As can be seen in Figures.10 and 2.68% of the harmonic spectrum, the source current total harmonic distortion has been reduced from 13.44 percent to 268 percent. Figure 11 shows the integrated system with the step-up converter's DC-link voltage control techniques. i) ANFIS with and without MPPT in PV-SAPF; ii) PI Figure 10. Harmonic spectrum: pre- and post-phase A source current correction. The transient response of various control algorithms to DC-link voltage is shown in Figure 11. TABLE 4. DC link voltage performance in SAPF with various control algorithms: (i) INC for MPPT in SAPF; (iii) ANFIS for MPPT in PV-SAPF and EINC; (iv) PI for MPPT in PV-SAPF and EINC; and (v) PI for MPPT in PV-SAPF and PSO. The results of the DC link voltage in SAPF when different control strategies are used are shown in Table 4. Better transient responsiveness with reduced overshoots and DC-link voltage fluctuations are provided by the EINC MPPT with the ANFIS-based PV-SAPF approach, which settles quicker than the PI-based method.

HARDWARE RESULTS AND DISCUSSION

To build a SAPF for reactive power compensation and harmonic reduction, it is necessary to carefully design and choose components such as DC bus capacitors, source and filter inductors, a voltage source inverter, and appropriate control circuits. The performance of the SAPF is impacted by the choices of processor speed, interface circuits, and sensor components. Table showing experimental validation utilized for SAPF system design parameters. 5. Artix-7 of the Vivado 2023.2 The DSP FPGA controller runs an algorithm that relies on reference frames in a synchronous manner.

TABLE 5. Design parameters of the experimental validation

Components	Parameter	Value
Grid	Source voltage (Phase voltage)	230 V,50 Hz
Filter	Inductance	5 mH
DC-link voltage	Capacitor	2200µF
Nonlinear load	Resistor and inductor	R=81Ω and L=12mH
Load	Resistive load	0.5KW to 1.5KW
	Inductive load	80mH to 160mH
Chromo PV simulator (model-62050H-600S)	Open circuit voltage, V_{OC} Short circuit current, I_{SC}	600V 6A

aiding the SAPF methodology. Each phase's load voltages and currents are sensed by the Hall Effect current sensor (HE100T01) and the voltage sensor (IC 7840), respectively. Also, the control and power

ISSN 2321-2152
www.ijmece.com
Vol 13, Issue 2, 2025

circuits are isolated using these transducers. In order to make good use of the FPGA's analogue channels, the sensor signals are first converted to a range of 0 to 5 V using a signal conditioning circuit. Information output lines provide the digital data to the field-programmable gate array (FPGA) processor from the 12-bit bipolar Analog to Digital (A/D) converters (IC AD7366) that these circuits produce. Using the synchrous reference theory as a foundation, the program is used to build the switching signals for IGBTs. In order for the drive function to work, the driver circuit (TLP 250 IC) must keep the minimum current constant. In order to generate switching pulses for the IGBT modules, four driver circuits are needed (SKM100GB12T4). In order to achieve SAPF, the SEMITRANS2fastIGBTModuleusesthe three-level diode clamped inverter. See the SAPF prototype model in action in Figure 12. A. SRF Theory Implementation in FPGAs In order to implement the SRF control strategy of SAPF in a modular way, the suggested study makes use of FPGA. The control performance is then continually monitored. Complete development of the controller has been carried out using an Artix-7 DSP FPGA. Figure 13 shows the overall schematic of the control strategies' modular design. To accomplish all of the controller operations, there are four modules: reference signal generation, synchronization, A/D conversion, positive sequence extractor, and switching pulses (PWM) module. 1) Comparable to the USB Module The A/D conversions are carried out by this module by use of an external ADC channel, which acquires consecutive bits. After the external ADC and FPGA have synchronized, the system transmits the 12-bit bipolar analog to digital converters (IC AD7366) that have been produced to the next module.

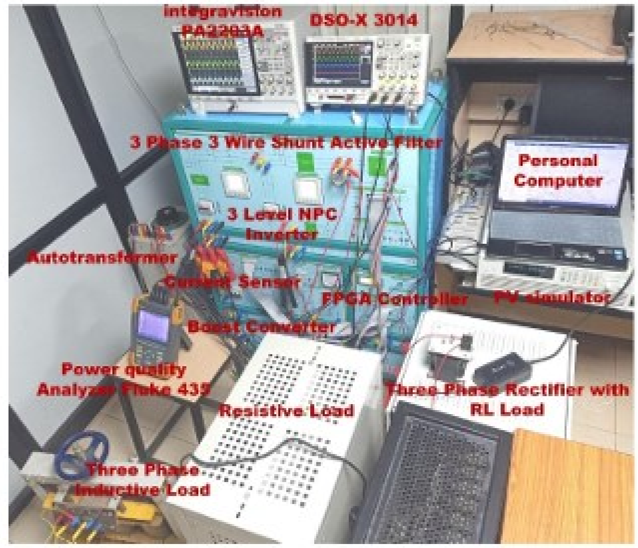

FIGURE 12. The SAPF was implemented using the SRF technique on the laboratory's experimental setup.

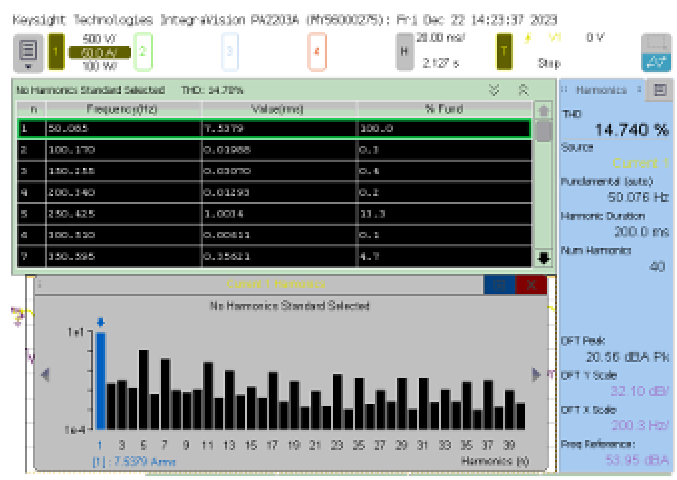

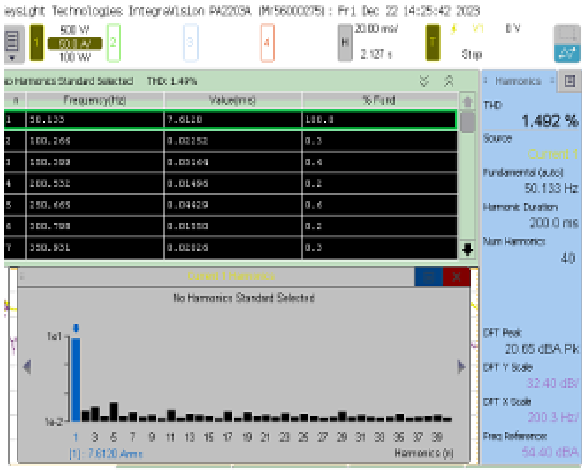

(b)

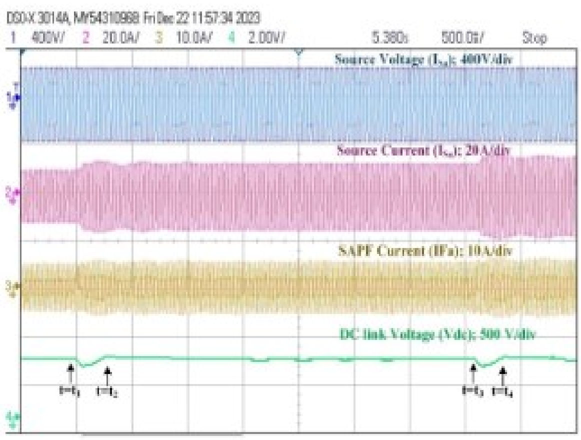

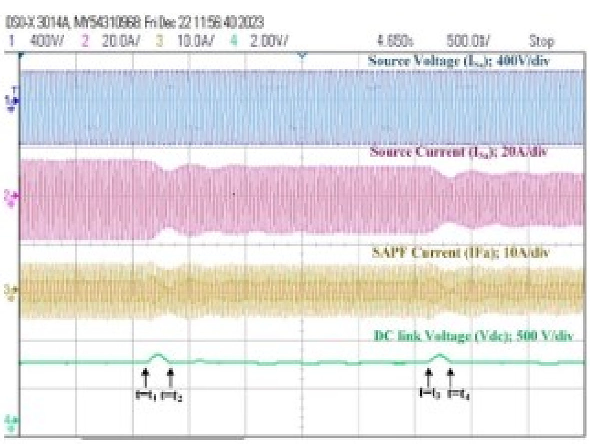

FIGURE 24. SAPF's reaction to a dynamic loading condition ranging from 0.5 KW to 1.5 KW (Phase-A). The three-level APF enhances harmonic distortion in both the load and source currents. A two-stage inverter takes three-phase currents and filter voltages and produces a sinusoidal source current by adjusting for harmonics. These demonstrate that the filter voltages and currents exhibit huge step sizes and harmonic content, in contrast to the three-level SAPF. Consequently, they make things more difficult for SAPF, which leads to losses for the contractor. Figure 26 (a) and (b) demonstrate that two-level inverter SAPF reduces the percentage of source current THD from 26% to 4.3%, while Figures 20 (a) and (b) show that three-level-based SAPF reduces it from 26% to 1.5%. F. How PV-Based SAPFs Fare Under Non-Linear Loads The diode bridge RL load was totally supported by the grid in the starting state, and the PV current at the output was zero. When 74 the 494 Figure 25 shows the response of SAPF (Phase-A) to a dynamic loading scenario including a change from 1.5 KW to 0.5 KW. Figures 14, 15, 16, and 17 depict the flow of electricity from the generator to the load as it operates. To create harmonic current, it adjusts for reactive power demand and NL load. Source current is enhanced from 5.05A to 5.35A, and total harmonic distortion (THD) is decreased from 26.00% to 1.5%. In the second scenario, the converter current stays constant, PV power is received, and the boost converter and NPC inverter are both switched on. The required value is achieved via the dc-link capacitor voltage (Vdc). In steady-state operation, the dual-purpose inverter supplies the reactive and harmonic components of the NL load current while also delivering real power from the solar array into the power conversion converter (PCC). PV is linked with the SAPF portion of the active power sent from PV-SAPF to the load. This keeps the a-phase PCC voltage in phase with the grid current. All three of these currents—source, load, and filter—are shown in Figure 27. The total harmonic distortion (THD) of the input current drops from 26.0% to 2.7%, as shown in Figure 29(a).

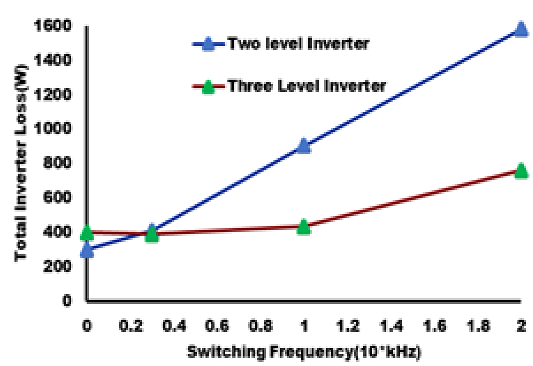

ISSN 2321-2152
www.ijmece.com
Vol 13, Issue 2, 2025

FIGURE 30. Comparative analysis of the overall losses between two-level and three-level inverters at different switching frequencies

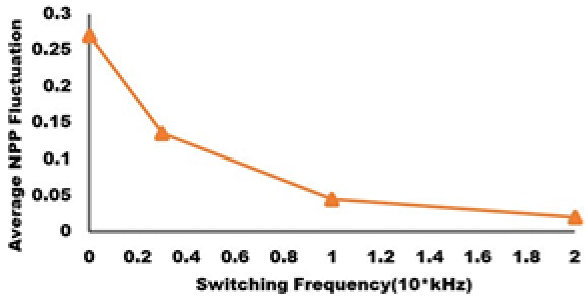

FIGURE 31. Two capacitor voltages vary with three level inverter switching frequency.

description of the 1200.0 V SEMITRANS2 (SKM100GB12T4) device. Each capacitor for the DC-link had a capacitance value of 2200µF, and the DC-bus voltage was set at 750.0 V. There was a considerable decrease in total inverter loss after the use of the control approach. As a result, the overall inverter loss is now 60% lower than it was with the two-level inverter, and it's around 54% lower than the loss shown in the scheme with greater switching frequencies. As shown in Equation 18, the average neutral point potential varies in response to changes in the modulation index, as seen visually in Figure 31. The voltage fluctuation in the architecture based on low-switching losses is about half of what it is in the topology based on high-switching losses. Depending on the voltage difference between the capacitors, this duty cycle change happens throughout the switching cycles.

$$V_{dc\ CapDiff} = \frac{V_{dc\ Cap\ upper} - V_{dc\ Cap\ lower}}{V_{dc}} \qquad (18)$$

The loss distribution of diodes and IGBTs, as well as the conduction and switching losses of two-level and three-level inverters, are shown in Figure 32 (a) and (b). A two-level inverter has a balanced distribution of losses in its upper and lower legs. Having said that, a three-level inverter's loss distribution isn't uniform. This is because the switching is changed often.

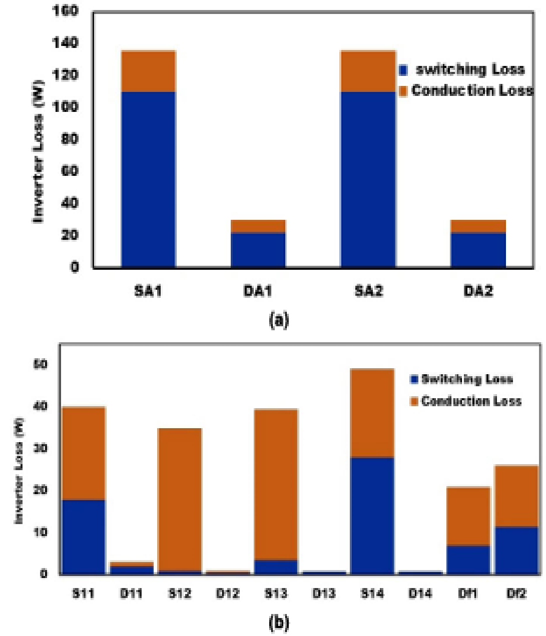

FIGURE 32. Conduction and switching losses of (a) Two-level inverter and (b) Three-level inverter

in a certain order such that the two DC-link capacitors continue to have identical voltages. Furthermore, compared to the outside switches, the conduction periods of the inner IGBT switches are much longer. Furthermore, for large modulation indices, antiparallel diode losses are almost nonexistent. This is because NPC diodes enable the load current to flow even when main power switches like S11 and S14 are turned off, thanks to their greater power sharing capabilities. Conduction losses clearly play a larger role in a three-level inverter than switching losses do in a two-level one. Figure 33 shows the system's efficiency in action; three-level NPC multilevel inverters outperform traditional inverters in terms of efficiency, mostly because they have lower switching losses. After comparing the two inverters, we find that the three-level Neutral Point Clamped inverter performs 4% better. Regardless of the load, it maintains an efficiency rate of 97.5%.

Conclusion

A three-level Neutral Point clamped voltage source inverter-based three-phase shunt active power filter for reactive power compensation and harmonic reduction in balanced and unbalanced nonlinear loads is suggested in this study. The filter is based on photovoltaic (PV) interface technology. The use of SRF theory and an ANFIS algorithm-based controller improves the SAPF's performance. The ANFIS controller maintains a steady DC link voltage and uses SRF theory to provide a reference current for correction. The model has been tested in a variety of settings, including real hardware and virtual ones. In terms of controlling voltage, reducing harmonics, and balancing loads, the suggested SAPF delivers good performance under balanced and unbalanced NL loads. In addition, there are no frequency fluctuations seen at PCC. The experimental findings reveal that it produces a total harmonic distortion (THD) of 26.0% before to correction, which drops to 1.5% after compensation for nonlinear loads. By changing the linear loads, a large number of observations are recorded and tabulated throughout the performance assessment of the proposed system under balanced linear load circumstances. Assuming R = 0.5 KW and L = 160 mH, the total harmonic distortion (THD) measured before adjustment is 14.740%, and it drops to 1.492% after compensation. The findings of the analysis of the suggested system's performance under dynamic load situations are similarly good. Additionally, the study is conducted to determine the feasibility of active power production by PV, and the results are confirmed under various supply scenarios. Compensation brings the power factor close to unity, and the resultant current THD fulfills the harmonic bounds of IEEE 519-1992.

REFERENCES

[1]. E. Koutroulis and F. Blaabjerg, ‘‘A new technique for tracking the global maximum power point of PV arrays operating under partial-shading con ditions,’’ IEEE J. Photovolt., vol. 2, no. 2, pp. 184–190, Apr. 2012, doi: 10.1109/JPHOTOV.2012.2183578.

[2]. J. Ahmed and Z. Salam, ‘‘A critical evaluation on maximum power point tracking methods for partial shading in PV systems,’’ Renew. Sustain. Energy Rev., vol. 47, pp. 933–953, Jul. 2015, doi: 10.1016/j.rser.2015.03.080.

[3]. O. Pinzón-Quintero, D. Gaviria-Ospina, A. Parrado-Duque, R. Rodríguez-Velásquez, and G. Osma-Pinto, ‘‘Assessment of power quality parameters and indicators at the point of common coupling in a low voltage power grid with photovoltaic generation emulated,’’ Electr. Power Syst. Res., vol. 203, Feb. 2022, Art. no. 107679, doi: 10.1016/j.epsr.2021.107679.

[4]. W. U. Rehman, A. R. Bhatti, A. B. Awan, I. A. Sajjad, A. A. Khan, R. Bo, S. S. Haroon, S. Amin, I. Tlili, and O. Oboreh-Snapps, ‘‘The penetration of renewable and sustainable energy in asia: A State-of-the-Art review on net-metering,’’ IEEE Access, vol. 8, pp. 170364–170388, 2020, doi: 10.1109/ACCESS.2020.3022738.

[5]. M. M. V. Cantarero, ‘‘Of renewable energy, energy democracy, and sustainable development: A roadmap to accelerate the energy transition in developing countries,’’ Energy Res. Social Sci., vol. 70, Dec. 2020, Art. no. 101716, doi: 10.1016/j.erss.2020.101716.

[6]. S.J. Pinto, G. Panda, and R. Peesapati, ‘‘An implementation of hybrid con trol strategy for distributed generation system interface using Xilinxsystem generator,’’ IEEE Trans. Ind. Informat., vol. 13, no. 5, pp. 2735–2745, Oct. 2017, doi: 10.1109/TII.2017.2723434.

[7]. S. Echalih, A. Abouloifa, I. Lachkar, A. E. Aroudi, Z. Hekss, F. Giri, and M. S. Al-Numay, ‘‘A cascaded controller for a grid-tied photovoltaic system with three-phase half-bridge interleaved buck shunt active power f ilter: Hybrid control strategy and fuzzy logic approach,’’ IEEE J. Emerg. Sel. Topics Circuits Syst., vol. 12, no. 1, pp. 320–330, Mar. 2022, doi: 10.1109/JETCAS.2022.3152535.

[8]. X. Liang and C. Andalib-Bin-Karim, ‘‘Harmonics and mitigation tech niques through advanced control in grid-connected renewable energy sources: A review,’’ IEEE Trans. Ind. Appl., vol. 54, no. 4, pp. 3100–3111, Jul. 2018, doi: 10.1109/TIA.2018.2823680.

[9]. S. Senguttuvan and M. Vijayakumar, ‘‘Solar photovoltaic system inter faced shunt active power filter for enhancement of power quality in three-phase distribution system,’’ J. Circuits, Syst. Comput., vol. 27, no. 11, Oct. 2018, Art. no. 1850166, doi: 10.1142/s0218126618501669.

[10]. W.Yuan,X.Yuan,L.Xu,C.Zhang,andX.Ma,‘‘ Harmoniclossanalysisof low-voltage distribution network integrated with distributed photovoltaic,’’ Sustainability, vol. 15, no. 5, p. 4334,Feb.2023,doi:10.3390/su15054334.

[11]. N. Debdouche, B. Deffaf, H. Benbouhenni, Z. Laid, and M. I. Mosaad, ‘‘Direct power control for three-level multifunctional voltage source inverter of PV systems using a simplified super-twisting

algorithm,'' Ener gies, vol. 16, no. 10, p. 4103, May 2023, doi: 10.3390/en16104103.

[12]. R. Boopathi and V. Indragandhi, ''Comparative analysis of control tech niques using a PV-based SAPF integrated grid system to enhance power quality,'' e-Prime Adv. Electr. Eng., Electron. Energy, vol. 5, Sep. 2023, Art. no. 100222, doi: 10.1016/j.prime.2023.100222.

[13]. T. M. T. Thentral, K. Vijayakumar, S. Usha, R. Palanisamy, T. S. Babu, H. H. Alhelou, and A. Al-Hinai, ''Development of control techniques using modified fuzzy based SAPF for power quality enhancement,'' IEEE Access, vol. 9, pp. 68396–68413, 2021, doi: 10.1109/ACCESS.2021.3077450.

[14]. A. A. Imam, R. S. Kumar, and Y. A. Al-Turki, ''Modeling and simulation of a PI controlled shunt active power filter for power quality enhancement based on P-Q theory,'' Electronics, vol. 9, no. 4, p. 637, Apr. 2020, doi: 10.3390/electronics9040637.

[15]. A. Bielecka and D. Wojciechowski, ''Stability analysis of shunt active power filter with predictive closed-loop control of supply current,'' Ener gies, vol. 14, no. 8, p. 2208, Apr. 2021, doi: 10.3390/en14082208.

[16]. S. Nyamathulla, D. Chittathuru, and S. M. Muyeen, ''An overview of multilevel inverters lifetime assessment for grid-connected solar photo voltaic applications,'' Electronics, vol. 12, no. 8, p. 1944, Apr. 2023, doi: 10.3390/electronics12081944.

[17]. U.-M. Choi, J.-S. Lee, F. Blaabjerg, and K.-B. Lee, ''Open-circuit fault diagnosis and fault-tolerant control for a grid-connected NPC inverter,'' IEEE Trans. Power Electron., vol. 31, no. 10, pp. 7234–7247, Oct. 2016, doi: 10.1109/TPEL.2015.2510224.

[18]. N. V. Kurdkandi, M. G. Marangalu, S. Mohammadsalehian, H. Tarzamni, Y. P. Siwakoti, Md. R. Islam, and K. M. Muttaqi, ''A new six-level transformer-less grid-connected solar photovoltaic inverter with less leakage current,'' IEEE Access, vol. 10, pp. 63736–63753, 2022, doi: 10.1109/ACCESS.2022.3182240.

[19]. N. V. Kurdkandi, M. G. Marangalu, O. Husev, A. Aghaie, M. R. Islam, Y. P. Siwakoti, K. M. Muttaqi, and S. H. Hosseini, ''A new seven level transformer-less grid-tied inverter with leakage current limitation and voltage boosting feature,'' IEEE J. Emerg. Sel. Topics Ind. Elec tron., vol. 4, no. 1, pp. 228–241, Jan. 2023, doi: 10.1109/JESTIE.2022. 3205546.

[20]. J.-S. Lee, R. Kwak, and K.-B. Lee, ''Novel discontinuous PWM method for a single-phase three-level neutral point clamped inverter with efficiency improvement and harmonic reduction,'' IEEE Trans. Power Electron., vol. 33, no. 11, pp. 9253–9266, Nov. 2018, doi: 10.1109/TPEL.2018.2794547.